

## Structural Characterization of Shielded Isomeric Europium Complexes with Metal–Metal Contact

Ga-Lai Law,<sup>†</sup> Ka-Leung Wong,<sup>\*‡</sup> Yang-Yi Yang,<sup>§</sup> Qiao-Yuan Yi,<sup>§</sup> Guohua Jia,<sup>‡</sup> Wing-Tak Wong,<sup>†</sup> and Peter A. Tanner<sup>\*‡</sup>

Department of Chemistry, The University of Hong Kong, Hong Kong S.A.R., People's Republic of China, Department of Biology and Chemistry, City University of Hong Kong, Tat Chee Avenue, Kowloon, Hong Kong S.A.R., People's Republic of China, and MOE Key Laboratory of Bioinorganic and Synthetic Chemistry, School of Chemistry & Chemical Engineering, Sun Yat-Sen University, Guangzhou 510275, People's Republic of China

Received June 14, 2007

New luminescent isomeric europium(III) complexes with carboxylic carbonyl group coordination (**I** and **II**) have been prepared by solvothermal synthesis using the ligand 2,2'-bipyridine-4,4'-dicarboxylic acid (bpdc), with the nonradiatively shielded Eu<sup>3+</sup> coordination sphere completed by dimethyl sulfoxide ligands. The room temperature IR spectra and Eu<sup>3+</sup> luminescence spectra do not provide a definitive distinction between **I** and **II**, but low-temperature luminescence can give a clear identification.

### Introduction

The choice of ligand for complexation plays a key role in constructing efficient luminescent lanthanide complexes. Two of the common requirements when choosing a ligand for coordination with lanthanide ions are the binding strength and the ultraviolet (UV) absorption properties of the ligand entity. Aromatic carboxylate ligands fulfill the above two basic criteria<sup>1–2</sup> as sensitizing agents for enhancing the luminescence of lanthanide ions because they can chelate the lanthanide metal ions tightly as well as display strong UV absorption. In particular, 2,2'-bipyridine-6,6'-dicarboxylic acid is a good antenna to sensitize emission from Tb<sup>3+</sup>.<sup>3</sup> The aqua complexes of the isomer 2,2'-bipyridine-4,4'-dicarboxylic acid (bpdc) with the three lanthanide ions Eu, Tb, and Gd have been characterized by luminescence spectroscopy, although a structural investigation was not carried out.<sup>4</sup> Because this ligand appears to be a promising antenna, we have further shielded the environment of Eu<sup>3+</sup> by removing

the OH<sub>2</sub> ligands in order to minimize nonradiative channels. Herein, we report the X-ray structure of europium(III) complexes with carbonyl group coordination using the ligand bpdc and demonstrate the subtle differences between the two isomers. The distinction between the isomers is readily accomplished from the low-temperature electronic emission spectra.

### Experimental Section

**Synthesis.** Direct reaction by solvothermal synthesis of europium trichloride with the ligand in dimethyl sulfoxide (DMSO) gave the polymeric europium complex with the two isomers [Eu<sub>2</sub>(bpdc)<sub>3</sub>(DMSO)<sub>4</sub>]<sub>n</sub>·6nH<sub>2</sub>O (**I**) and [Eu<sub>2</sub>(bpdc)<sub>3</sub>(DMSO)<sub>4</sub>]<sub>n</sub>·2nDMSO·2nH<sub>2</sub>O (**II**) (Figure 1). A mixture of EuCl<sub>3</sub>·6H<sub>2</sub>O, 2,2'-bipyridine-4,4'-dicarboxylic acid (bpdc; Figure S1 in the Supporting Information), and DMSO with a mole ratio of 1:1:1500 was stirred for 0.5 h and then sealed in a Teflon-lined autoclave. The mixture was heated at 100 °C for 2 days. After cooling to room temperature, colorless crystals were obtained on the walls of the flask and on the bottom, together with a small amount of precipitate (hereafter labeled as **PPT**). The crystals were removed, recrystallized, and then air-dried (isomer **I**). Isomer **II** was obtained from the mother solution after filtering out the mixture to remove the small amount of precipitate, and it also crystallized as a colorless block crystal (yield: **I**, 46%; **II**, 28%). The reaction was then repeated over the longer time period of 5 days. This resulted in a mixture without a precipitate, where **I** was again found on the container walls. Isomer **II** was obtained from slow evaporation of the mother solution over a few days because the crystal contains a higher proportion of DMSO. This reaction yielded different ratios of the two isomers (**I**, 23%; **II**,

\* To whom correspondence should be addressed. E-mail: klwong@cityu.edu.hk (K.-L.W.), bhtan@cityu.edu.hk (P.A.T.).

<sup>†</sup> The University of Hong Kong.

<sup>‡</sup> City University of Hong Kong.

<sup>§</sup> Sun Yat-Sen University.

- (1) Lukeš, I.; Kotek, J.; Vojtisek, P.; Hermann, P. *Coord. Chem. Rev.* **2001**, *216–217*, 287.
- (2) Beerby, A.; Bushby, L. M.; Maffeo, D.; Williams, J. A. *J. Chem. Soc., Dalton Trans.* **2002**, 48.
- (3) Bünzli, J.-C. G.; Charbonnière, L. J.; Ziessel, R. F. *J. Chem. Soc., Dalton Trans.* **2000**, 1917.
- (4) Calefi, P. S.; Ribeiro, A. O.; Pires, A. M.; Serra, O. A. *J. Alloys Comps.* **2002**, *344*, 285.

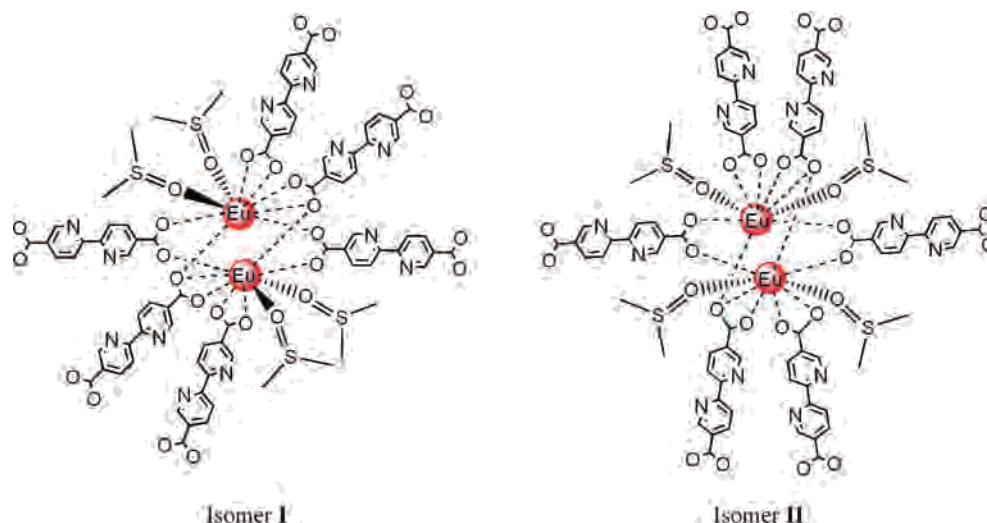


**Figure 1.** Structures of the europium isomers **I** (left) and **II** (right).

**Table 1.** Crystallographic and Data Collection Parameters for Isomers **I** and **II**

	<b>I</b>	<b>II</b>
$M_w$	1451.09	767.64
shape	block	block
color	colorless	colorless
$a$ (Å)	12.390(3)	10.0895(6)
$b$ (Å)	13.795(4)	11.4162(6)
$c$ (Å)	13.830(4)	13.6578(8)
$\alpha$ (deg)	115.769(4)	86.774(1)
$\beta$ (deg)	93.914(5)	72.594(1)
$\gamma$ (deg)	106.918(4)	78.675(1)
$V$ (Å <sup>3</sup> )	1983.8(9)	1471.89(15)
$D_{\text{calc}}$ (g cm <sup>-3</sup> )	1.215	1.732
cryst syst	triclinic	triclinic
space group	$P\bar{1}$	$P\bar{1}$
$Z$ value	1	2
$2\theta_{\text{max}}$	55.2	52.24
no. of collected reflns	8440	5651
no. of unique reflns	7222	4718
$R_{\text{int}}$	0.028	0.031
$R$ [ $I > 2.00\sigma(I)$ ]	0.072	0.038
GOF	1.051	1.045

34%). ESIMS: isomer **I**,  $m/z$  639,  $2\text{H}_3\text{BPDC} + 1\text{Eu}$ ; isomer **II**,  $m/z$  637,  $2\text{H}_3\text{BPDC} + 1\text{Eu}$ .

**Photophysical Data.** The UV–vis absorption spectra of the europium complexes were recorded using a HP UV-8453 spectrophotometer in the range from 200 to 1100 nm in MeOH at 298 K. The room temperature luminescence spectra were excited by the 355 nm line of a Continuum Nd:YAG laser. Room temperature excitation spectra were recorded using a Jobin-Yvon TCSPC system. The low-temperature emission spectra were recorded at a resolution of 2–4 cm<sup>-1</sup> by a back-illuminated SpectraMM CCD detector in an Acton 0.5 m monochromator having a 1200 groove mm<sup>-1</sup> grating blazed at 500 nm and a 600 groove mm<sup>-1</sup> grating blazed at 750 nm. The sample was housed in an Oxford Instruments closed-cycle cryostat and was excited by an Optical Parametric oscillator (Panther) pumped by the third harmonic of a Surelite Nd:YAG pulsed laser. FT-IR absorption spectra were recorded by a Perkin-Elmer 2000 spectrometer using KBr disks.

## Results and Discussion

**Crystal Structures.** The crystallographic and data collection parameters for **I** and **II** are listed in Table 1. Each monomer unit in **I** consists of two Eu ions, three bpdC

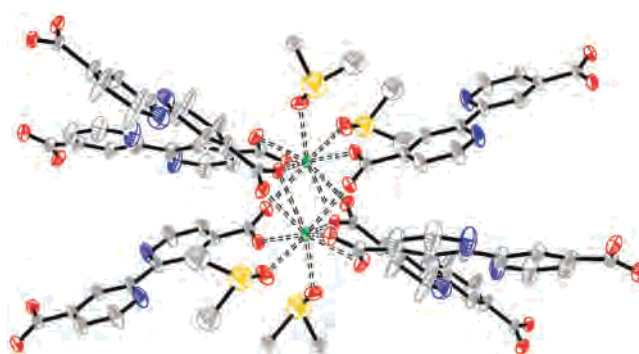


**Figure 2.** ORTEP drawing of isomer **I**.

ligands, and four DMSO solvates (Figure 2). From the X-ray crystallographic information, the asymmetric unit contains only half of the monomer unit; i.e., the two Eu atoms are equivalent. These units are hydrogen-bonded into a three-dimensional array (Figure 3). Each Eu<sup>3+</sup> ion is coordinated to nine O atoms: seven O atoms from five bpdC ligands and two O atoms from two DMSO ligands in a distorted monocapped square antiprism. The bottom square is composed of atoms O1, O2\*, O3, and O4\* (with the maximum deviation from the mean plane being 0.113 Å (O3)); \* = symmetry code 1 - x, 1 - y, 1 - z and capped by atom O3\*. The top square is composed of the atoms O5, O6, O7, and O8, with the maximum deviation from the mean plane being 0.114 Å (O6). The two mean planes are nearly parallel, with a dihedral angle of 4.47°. As a result, the monomer unit appears as a twisted four-layer square antiprism. The Eu–O distances are in the usual range of 2.374(6)–2.752(6) Å. Two Eu atoms are held closely together by four bridging bpdC ligands, with the distance Eu⋯Eu = 4.128 Å, which is rather long for a quadruply bridged Eu<sup>3+</sup>⋯Eu<sup>3+</sup> separation, although it is much shorter than the 6.51 Å Tb<sup>3+</sup>–Tb<sup>3+</sup> separation in  $[\text{Tb}_2(\text{bpdC})_3(\text{H}_2\text{O})_3] \cdot 2\text{H}_2\text{O} \cdot 2\text{MeOH}$ .<sup>3</sup>

Isomer **II** has the same number of bpdC and DMSO ligands and similar coordination but with different numbers and types of solvates in the lattice (Figures 4 and 5). As in **I**, the Eu<sup>3+</sup> metal center in **II** also shows a distorted monocapped square-antiprism geometry. With O1, O2, O7, and O8 as the bottom

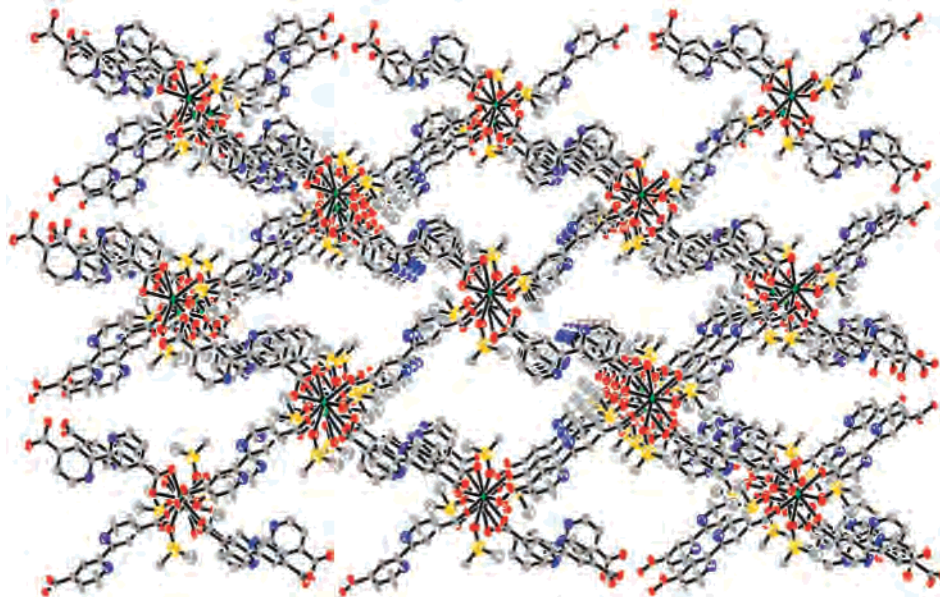


Figure 3. Packing diagram of isomer I.

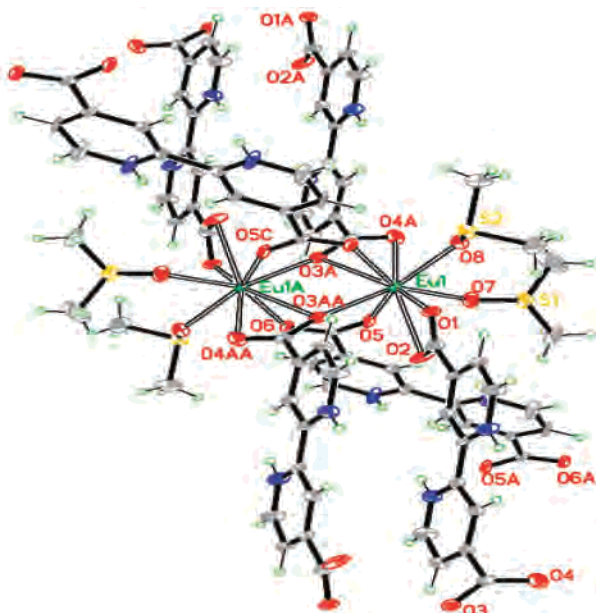


Figure 4. ORTEP drawing of isomer II.

square and O3<sup>i</sup>, O4<sup>ii</sup>, O5, and O6<sup>iii</sup> as the top square, which is capped by atom O3<sup>ii</sup> (symmetry codes: i, 2 - x, 1 - y, 1 - z; ii, x - 1, y, 1 + z; iii, 1 - x, 1 - y, 2 - z). The Eu...Eu distance of 4.090 Å is slightly shorter (0.03 Å) than that of isomer I. The Eu-O distances are in the range of 2.345(4)–2.695(4) Å and are slightly shorter (0.03–0.06 Å) than those in isomer I.

In isomer I, the carboxylic acid groups are all nearly orthogonal to each other (with dihedral angles of 44.83°, 80.08°, and 84.30°), whereas the pyridyl rings are only slightly twisted from their respective/connecting carboxylic acid groups in the range of only 14–23°. As a result, there is minimum overlapping between nearby/adjacent bpdc ligands, so that the only possible interactions are C-H... $\pi$  (e.g., H3B\*...N3-py-ring centroid = 3.124 Å; H4A\*...N3-py-ring centroid = 3.538 Å). However, in isomer II, the

carboxylic acid groups are closer to orthogonality than those in I (with dihedral angles of 65.57°, 76.25°, and 86.15°, respectively). Furthermore, there is a much larger dihedral angle (58.04°) between the C12/O3/O4 carboxylic acid group and its attached N2-py-ring. This significant twisting results in the parallel stacking of N2-py-ring and the neighboring N1-py-ring (the dihedral angle between these two py rings is only 4.83°, with the centroid-to-plane distance = ~3.467 Å). This enhanced  $\pi$ ... $\pi$  interaction results in more efficient packing in the unit cell (Figures S3 and S4 in the Supporting Information), with a significant reduction in the cell volume (1471 Å<sup>3</sup> in II vs 1984 Å<sup>3</sup> in I), despite the presence of one DMSO and one H<sub>2</sub>O in I versus three H<sub>2</sub>O in II per monomer unit. There exist closer Eu<sup>3+</sup>...Eu<sup>3+</sup> interactions and smaller Eu-O distances in II as compared with I.

The three bpdc ligands show different coordination modes (Figure S9 in the Supporting Information). One acts only as a bis-bidentate chelate, bridging to two Eu<sup>3+</sup> ions only. The second type is a tetradentate chelate, bridging to four different Eu<sup>3+</sup> ions instead of two. The third type of coordination is a combination of both: a hexadentate chelate, bridging to four Eu<sup>3+</sup> ions. The combination of these three types of coordination builds the complex polymer into a three-dimensional lattice.

**Room Temperature IR and Electronic Spectra of I and II.** The FT-IR spectra of I and II are very similar, as shown in Figure 6. Both spectra present a strong broad feature peaking at ~3375 cm<sup>-1</sup> due to hydrogen-bonded water. The region between 1608 and 1544 cm<sup>-1</sup>, comprising aromatic ring stretching and asymmetric carboxylate modes, is similar for I and II except that isomer I exhibits a prominent shoulder at 1679 cm<sup>-1</sup>, which is absent in II. The strongest band in each spectrum is the symmetric carboxylate stretch coupled to the asymmetric CH<sub>3</sub> deformation at 1410 cm<sup>-1</sup>. The S=O stretch in neat DMSO peaks at 1044 and 1058

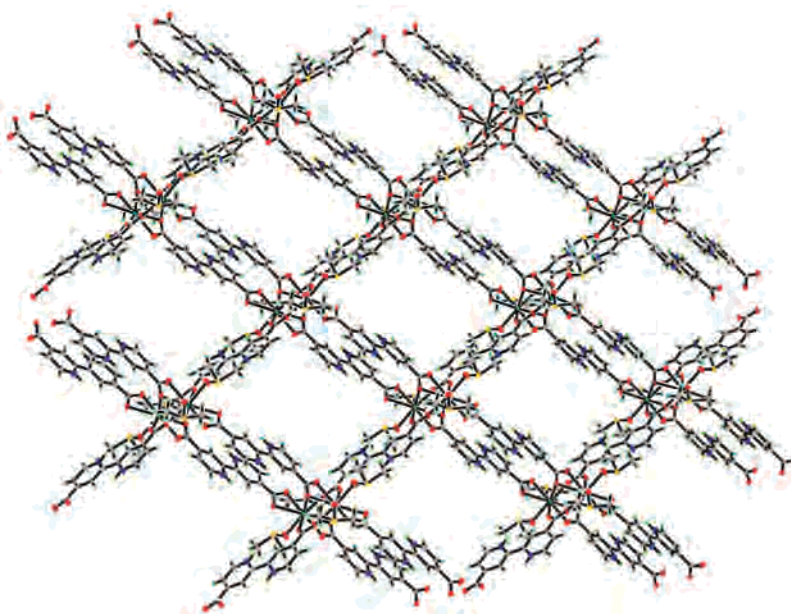


Figure 5. Packing diagram of isomer **II**.

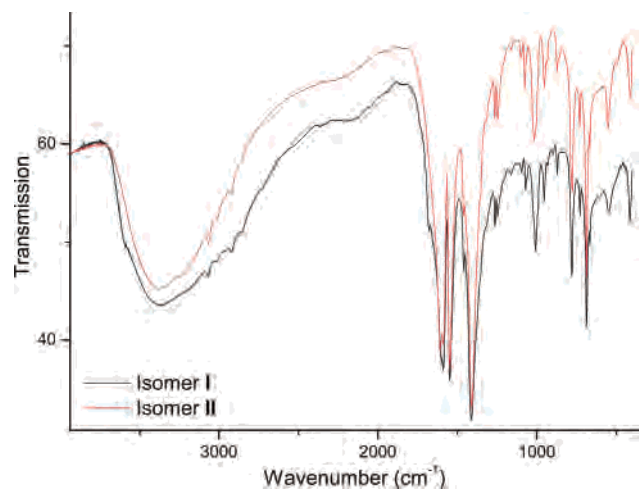


Figure 6. FT-IR spectra of isomers **I** and **II**.

$\text{cm}^{-1}$ .<sup>5</sup> It is lowered to  $\sim 950 \text{ cm}^{-1}$  upon complexation,<sup>6</sup> and there are medium-intensity bands at  $954 \text{ cm}^{-1}$  in the IR spectra of both **I** and **II**. Thus, as mentioned above, the differences in the FT-IR spectra of **I** and **II** are very minor, as exemplified, for example, by the additional shoulders at  $937$  and  $785 \text{ cm}^{-1}$  in **II**. Such differences are not readily rationalized in descriptive terms.

The solid-state electronic absorption spectra of the ligand and of the complexes display features at  $330$  and  $<250 \text{ nm}$  that are very similar (Figure S7 in the Supporting Information). The room temperature emission spectra of **I** and **II** under  $355 \text{ nm}$  laser excitation into the ligand antenna are displayed in Figure 7 and exhibit the characteristic  ${}^5\text{D}_0 \rightarrow {}^7\text{F}_J$  ( $J = 0, \dots, 4$ ) transitions of  $\text{Eu}^{3+}$ . Notably, the  ${}^5\text{D}_0 \rightarrow {}^7\text{F}_4$  transition, whose intensity is governed by the Judd–Ofelt parameter  $\Omega_4$ , which is mainly dependent upon “long-range”

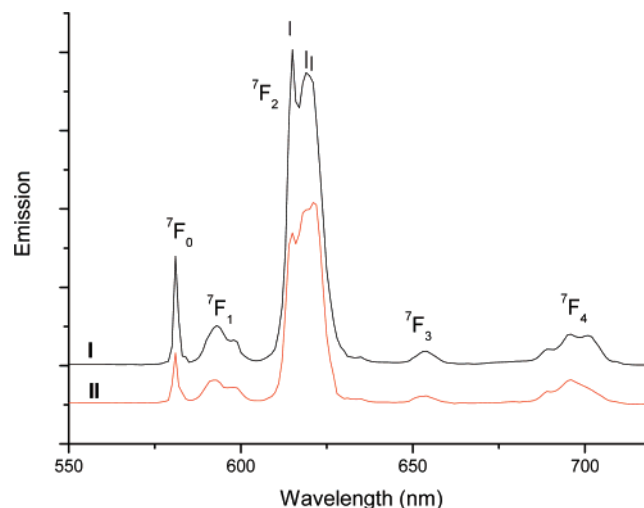


Figure 7.  $355 \text{ nm}$  excited-state room temperature emission spectra of **I** and **II** between  $550$  and  $730 \text{ nm}$ .

effects,<sup>7</sup> is fairly prominent. Because the site symmetry of  $\text{Eu}^{3+}$  is  $C_1$  and the two  $\text{Eu}^{3+}$  ions in the unit cell are related by the center of symmetry, the  $J$  degeneracies of the energy levels are completely removed so that one, three, and five bands are expected for the luminescence transitions from  ${}^5\text{D}_0$  to the terminal  ${}^7\text{F}_0$ ,  ${}^7\text{F}_1$ , and  ${}^7\text{F}_2$  multiplets, respectively. In fact, the spectral features are only partially resolved at room temperature so that the number of features is somewhat fewer, as shown by the three ticks for the  ${}^5\text{D}_0 \rightarrow {}^7\text{F}_2$  transition, for example. The exception is the  ${}^5\text{D}_0 \rightarrow {}^7\text{F}_0$  transition, where the one sharp band is observed. This is consistent not only with  $C_1$  site symmetry of  $\text{Eu}^{3+}$  but also with the presence of only one type of  $\text{Eu}^{3+}$  ion in the unit cell. As expected, the room temperature spectra of isomers **I** and **II** are very similar, particularly concerning the band energies. However, just as for the IR absorption spectra, the

(5) Fawcett, W. R.; Kloss, A. A. *J. Phys. Chem.* **1996**, *100*, 2019.

(6) Cotton, F. A.; Francis, R.; Horrocks, W. D. *J. Phys. Chem.* **1960**, *64*, 1534.

(7) Oomen, E. W. J. L.; Dongen, A. M. A. *J. Non-Cryst. Solids* **1989**, *111*, 203.

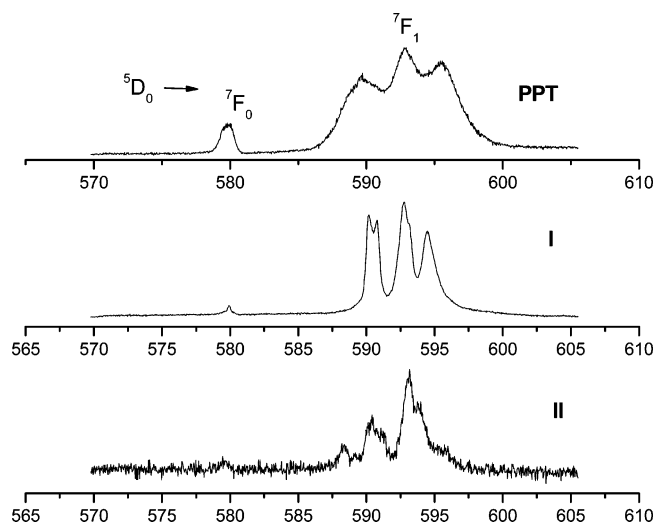


**Figure 8.** Comparison of the 457 nm excited-state 10 K luminescence spectra of PPT, **I**, and **II** between 570 and 605 nm.

minor differences that are present in the relative intensities of bands may not be considered definitive enough to confirm the identity of each isomer.

The room temperature solid-state luminescence excitation spectra of **I** and **II** were recorded by monitoring the  ${}^5D_0 \rightarrow {}^7F_2$  emission, and the spectra are shown in Figure S8 in the Supporting Information. The spectra of **I** and **II** are similar and exhibit maxima at 315 nm. This wavelength is near the maximum in the absorption spectra of DMSO solutions of **I** and **II** and corresponds to the ligand singlet–singlet transition. A lower energy shoulder is apparent in the excitation spectra at 376 nm.

**10 K Luminescence Spectra of I and II.** In order to gain a clearer distinction between **I** and **II**, the luminescence spectra were recorded under selective excitations at 10 K. The spectrum of the initial precipitate (PPT) was also recorded, and the comparison is displayed in Figure 8 for the 457 nm excited-state spectrum in the region of the  ${}^5D_0 \rightarrow {}^7F_{0,1}$  transitions. The impure nature of the initial precipitate (PPT) is manifested by the breadth of the spectral features. Isomers **I** and **II** are clearly differentiated, and the greater noise level for **II** is a consequence of the very small sample amount. Spectral features in **II** are generally blue-shifted relative to those in **I**, and the crystal-field splittings of the  ${}^7F_1$  levels differ considerably. The  ${}^5D_0 \rightarrow {}^7F_0$  electronic origins are at different energies: 17 243 and 17 257  $\text{cm}^{-1}$  in **I** and **II**, respectively. The most prominent  ${}^5D_0 \rightarrow {}^7F_1$  bands are at 16 925, 16 870, and 16 820  $\text{cm}^{-1}$  in **I**, whereas they are at 16 998, 16 937, and 16 860  $\text{cm}^{-1}$  in **II**. The major difference in the 10 K spectra compared with the room temperature spectra (Figure 7) is the smaller relative intensity of the  ${}^5D_0 \rightarrow {}^7F_0$  transition for both **I** and **II**, which may indicate changes in the  $\text{Eu}^{3+}$  site symmetry or less thermal disorder. Also, more than three bands are observed for the  ${}^5D_0 \rightarrow {}^7F_1$  transition region. This could be a consequence of (i) the resonance coupling of the excited-state electronic crystal-field levels with low-energy vibrational excitations of the electronic ground state, for example, as for the simpler

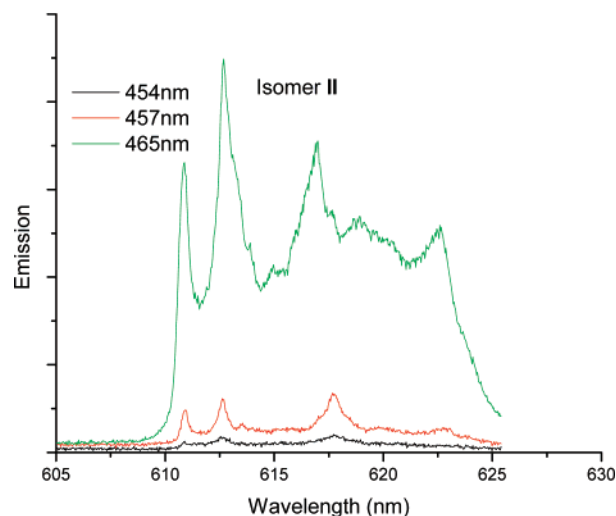
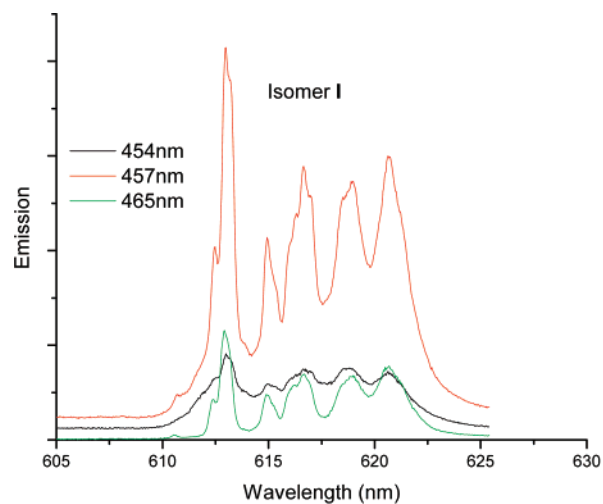


**Figure 9.** 10 K emission spectra of **I** and **II** in the region of the  ${}^5D_0 \rightarrow {}^7F_2$  transition between 606 and 625 nm under 454, 457, and 465 nm excitation wavelengths.

system  $\text{Eu}[\text{Co}(\text{CN})_6] \cdot 4\text{H}_2\text{O}$ ,<sup>8</sup> and/or (ii) the presence of impurities. We discount further reasons for the presence of “additional” bands such as the nonequivalence of the two  $\text{Eu}^{3+}$  sites in the unit cell or the Davydov splitting of the electronic transitions. If the possibility ii is correct, then the spectra recorded using several other laser excitation energies would show different relative intensities of bands. In fact, as shown for the  ${}^5D_0 \rightarrow {}^7F_2$  spectral region of **I** and **II** (Figure 9), there are more than five bands in this region, even taking into account the different relative intensities of some weaker features under 454, 457, and 465 nm excitation wavelengths. Thus, although the multicrystalline samples chosen for the recording of low-temperature luminescence spectra did contain some minor impurities, a clear distinction of isomers **I** and **II** from their emission spectra could be achieved. In view of the presence of more than  $2J + 1$  bands for the  ${}^5D_0 \rightarrow {}^7F_{1,2}$  transitions due to both i and ii, we do not attempt a crystal-field analysis of the energy levels.

(8) Zhou, X. J.; Duan, C. K.; Tanner, P. A. *J. Phys. Chem. Solids* **2007**, in press (doi 10.1016/j.jpcs.2007.05.023).

## Conclusions

The ligand bpdc has been employed to synthesize luminescent europium complexes without aqua ligands in the nine-atom coordination sphere. The two isomers exhibit polymeric structures but comprise the same ligands in their first coordination spheres. The IR absorption and room temperature electronic emission spectra of the two isomers do not permit a clear distinction between the isomers, but there are significant differences in the low-temperature electronic emission spectra that distinguish **I** and **II**. The Eu••Eu distances in the complexes are 4.1 Å. These distances are comparable to those in Eu<sup>3+</sup> complexes with thiophenyl-derivatized nitrobenzoato antennae (3.98–5.05 Å)<sup>9</sup> and the ethyl 4,4,4-trifluoroacetoacetate tetramer complex (3.66–4.54 Å)<sup>10</sup> but rather shorter than that in the 2-pyrazinecarboxylic acid complex (6.58 Å).<sup>11</sup>

**Acknowledgment.** Financial support of this work is acknowledged under the Hong Kong University Research

Grants Council Central Earmarked Research Grant CityU 102607 and the Nature National Science Foundation of China (Grant 50572125). K.-L.W. acknowledges the Research Scholarship Enhancement Scheme from City University of Hong Kong.

**Supporting Information Available:** Crystal structure diagrams, UV–vis spectra, and a ligand IR spectrum. This material is available free of charge via the Internet at <http://pubs.acs.org>. Crystallographic information is available as CCDC 644572 (isomer **I**) and 648228 (isomer **II**) from the Cambridge Crystallographic Data Centre (CCDC). These data may be obtained free of charge from the CCDC via the web link [www.ccdc.cam.ac.uk/data\\_request/cif](http://www.ccdc.cam.ac.uk/data_request/cif).

IC701162J

(9) Viswanathan, S.; de Bettencourt-Dias, A. *Inorg. Chem.* **2006**, *45*, 10138.

(10) Souza, A. P.; Paz, F. A. A.; Freire, R. O.; Carlos, L. D.; Malta, O. L.; Alves, S., Jr.; de Sà, G. F. *Inorg. Chem.* **2007**, in press (doi 10.1021/ic070335w).

(11) Eliseeva, S. V.; Mirzov, O. V.; Troyanov, S. I.; Vitukhnovsky, A. G.; Kuzmina, N. P. *J. Alloys Compds.* **2004**, *374*, 293.